Electronic Supplementary Material (ESI) for Dalton Transactions.

An indirect generation of 1D M^{II}-2,5-dihydroxybenzoquinone coordination polymers, their structural rearrangments and generation of materials with a high affinity for H_2, CO_2 and CH_4†

Brendan F. Abrahams,[a]* A. David Dharma,[a] Brendan Dyett,[a] Timothy A. Hudson,[a] Helen Maynard-Casely,[b] Christopher J. Kingsbury,[a] Laura J. McCormick,[a] Richard Robson,[a]* Ashley L. Sutton[a] and Keith F. White[a]

Electronic Supplementary Information

[a]School of Chemistry, University of Melbourne, Parkville, Victoria 3010, Australia Email: bfa@unimelb.edu.au; r.robson@unimelb.edu.au; Fax: +61 3 9347 5180; Tel: +61 3 8344 0341

[b]Bragg Institute, Australian Nuclear Science and Technology Organisation, Locked Bag 2001, Kirrawee DC, New South Wales 2234, Australia

S.1 Synthetic and crystallographic details

1,2,4,5-Tetrahydroxybenzene

1,2,4,5-tetrahydroxybenzene was prepared according to the literature method [R1]. Granulated tin (10.0 g, 84.2 mmol) was added to a suspension of H_2dhbq (10.0 g, 71.4 mmol) in refluxing HCl (32 %, 220 mL). The mixture was stirred for approximately 20 minutes, during which time the solution developed to a transparent brown solution. The excess tin was removed from the hot solution, which was then cooled to 4 °C. Colourless needle-like crystals of H_4dhbq were collected and washed with copious amounts of glacial acetic acid then finally with a small amount of chilled acetonitrile. The remaining solid was stored under N_2.

Cis-Mg(dhbq)(H_2O)$_2$. 2.5MeOH. 2H_2O – Crankshaft chains

A solution containing the reduced form of 2,5-dihydroxybenzoquinone (1,2,4,5-tetrahydroxybenzene) (50 mg, 0.35 mmol) in MeOH (15 mL) was added to an aqueous solution (5 mL) that contained $Mg(OAc)_2 \cdot 4H_2O$ (76 mg, 0.35 mmol). The reaction mixture was subsequently capped and allowed to stand at room temperature. Overnight small red block-like crystals separated from the solution.

Elemental analysis on an air dried sample (%) found: C 34.5, H 3.3 for Mg(dhbq)(H_2O)$_2$. 0.6H_2O calc'd (%); C 34.4, H3.4.

Cis-Zn(dhbq)(H_2O)$_2$. 1.5EtOH. 2H_2O

An solution containing ethanol (180 mL) and the reduced form of 2,5-dihydroxybenzoquinone (1,2,4,5-tetrahydroxybenzene) (600 mg, 4.22 mmol) was combined with an aqueous solution (30 mL) that consisted of $Zn(NO_3)_2 \cdot 6H_2O$ (1.260 g, 4.23 mmol). The reaction mixture was capped and left to stand; subsequently, small, pink crystals separated from the solution.

Yield on filtering: 447 mg.

Elemental for fresh material (%) found: C 30.00 H 2.63 for Zn(dhbq)(H_2O)$_2$ calc'd (%) C 30.09, H 2.53.

Elemental for material after drying at 180 °C (%) found: C 34.32, H 1.18, for $Zn(dhbq)(H_2O)_{0.4}$ calc'd (%) C 34.21, H 1.34

Trans-Mg(dhbq)(H_2O)$_2$ for single-crystal analysis

An aqueous solution (2 mL) containing the reduced form of 2,5-dihydroxybenzoquinone (1,2,4,5-tetrahydroxybenzene) (0.0645 g, 0.454 mmol) was combined with an aqueous solution (1 mL) that consisted of $Mg(OAc)_2{\cdot}4H_2O$ (0.09 g, 0.420 mmol). The reaction mixture was capped. Upon standing overnight small, cherry red crystals separated from the solution.

Trans-Zn(dhbq)(H_2O)$_2$ for single-crystal analysis

An aqueous solution (3 mL) containing the reduced form of 2,5-dihydroxybenzoquinone (1,2,4,5-tetrahydroxybenzene) (0.035 g, 0.246 mmol) was combined with an aqueous solution (3 mL) that consisted of $Zn(NO_3)_2{\cdot}6H_2O$ (0.62 g, 0.208 mmol). The reaction mixture was capped. Upon standing overnight small, red crystals separated from the solution.

General crystallographic details

Prior to X-ray data collections, a selected crystal was transferred directly from their mother liquor to protective oil. Crystallographic data were collected at 130 K on a SuperNova Oxford Diffractometer, fitted with a CuKα (1.54184 Å) X-ray source. Numerical absorption corrections were carried out using a multifaceted crystal model, and the ABSPACK routine within the CrysAlis software package. Crystallographic analysis was performed using the WinGX suite of programs. [R2] Crystal structures were solved by direct methods and refined using a full-matrix least squares procedure. Structural solutions and refinements were performed using either SHELX97 or SHELX14. [R3]

The crystals of both *cis*-$Mg(dhbq)(H_2O)_2$. 2.5MeOH. $2H_2O$ and *cis*-$Zn(dhbq)(H_2O)_2$. 1.5EtOH. $2H_2O$ possess large solvent accessible void regions. Within these void regions two non-coordinated water molecules are well located and were refined with anisotropic displacement parameters. The remainder of the void in each crystal is occupied by highly disordered solvent molecules. Attempts to model the solvent in each of the crystals resulted in an unstable refinement. As a result the *SQUEEZE* routine from the crystallographic program PLATON [R4] was employed to produce a modified data set in which the contribution of the disordered solvent was removed. In the case of the Mg-analogue, the calculated volume of the void and electron density removed was consistent with presence of twenty methanol molecules per unit cell. The *SQUEEZE* data obtained from the Zn-analogue was consistent with the presence of 12 ethanol molecules per unit cell.

S.2 Powder XRD Patterns

Powder x-ray diffraction data for the magnesium compounds and the dehydrated Zn(dhbq) were collected on the powder diffraction beamline at the Australian synchrotron [R6]. The samples were loaded into a 0.3 mm quartz capillary and mounted on the powder diffraction beamline. The experiments were undertaken with a wavelength of either 0.7796 or 0.8262 Å (1). The wavelengths were refined from a NIST SRM LaB_6-660b standard. Data were collected using the Mythen microstrip detector [R6] from 3 – 83° two theta. To cover the gaps between detector modules, 2 datasets were collected with the detector set 0.5° apart and then merged to a single dataset. In each case, the two theta values have been converted from the experimental X-ray wavelength used at the synchrotron to a value corresponding to a wavelength of 1.54145 Å. PXRD data obtained on the two zinc compounds: *cis*-Zn(dhbq)$(H_2O)_2$ and its subsequent air dried solid *trans*-Zn(dhbq)$(H_2O)_2$ were collected on an Supanova Oxford diffractometer fitted with a CuKα (1.54184 Å) x-ray source.

Powder data generated from a slurry of *cis*-Mg(dhbq)$(H_2O)_2$ and a subsequently air dried sample were processed using the powder analysis program Expo2014 [R7]. The peaks were indexed and unit cell parameters were extracted on the basis of the found peaks using the N-Treor process. The profiles from unit cell parameters with the highest ‘M20 score’ were then fitted to the experimental data using Le-Bail refinement cycles. The unit cell parameters along with the fitted profiles as well as the *Rwp* and *Rp* refinement statistics are shown below.

Cis-Mg(dhbq)(H_2O)$_2$ crankshaft chains

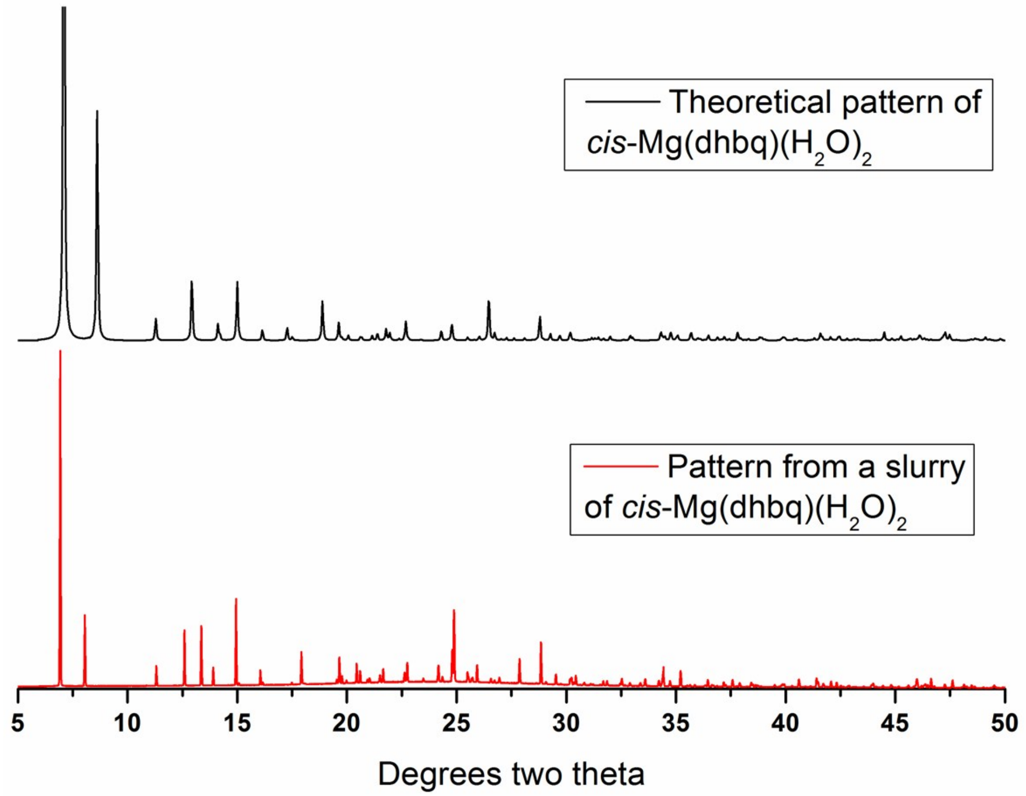

Figure S 1: Powder patterns of a slurry of *cis*-Mg(dhbq)(H_2O)$_2$ (red) and the powder pattern generated from the single crystal data of *cis*-Mg(dhbq)(H_2O)$_2$ (black).

Table S 1. Unit cell parameters extracted from a slurry of *cis*-Mg(dhbq)(H_2O)$_2$

M20 score	81.0
System	Monoclinic
a (Å)	22.413
b (Å)	15.609
c (Å)	9.268
β °	101.298
Vol (Å^3)	3179.6
Rwp (%)	2.64
Rp	1.80

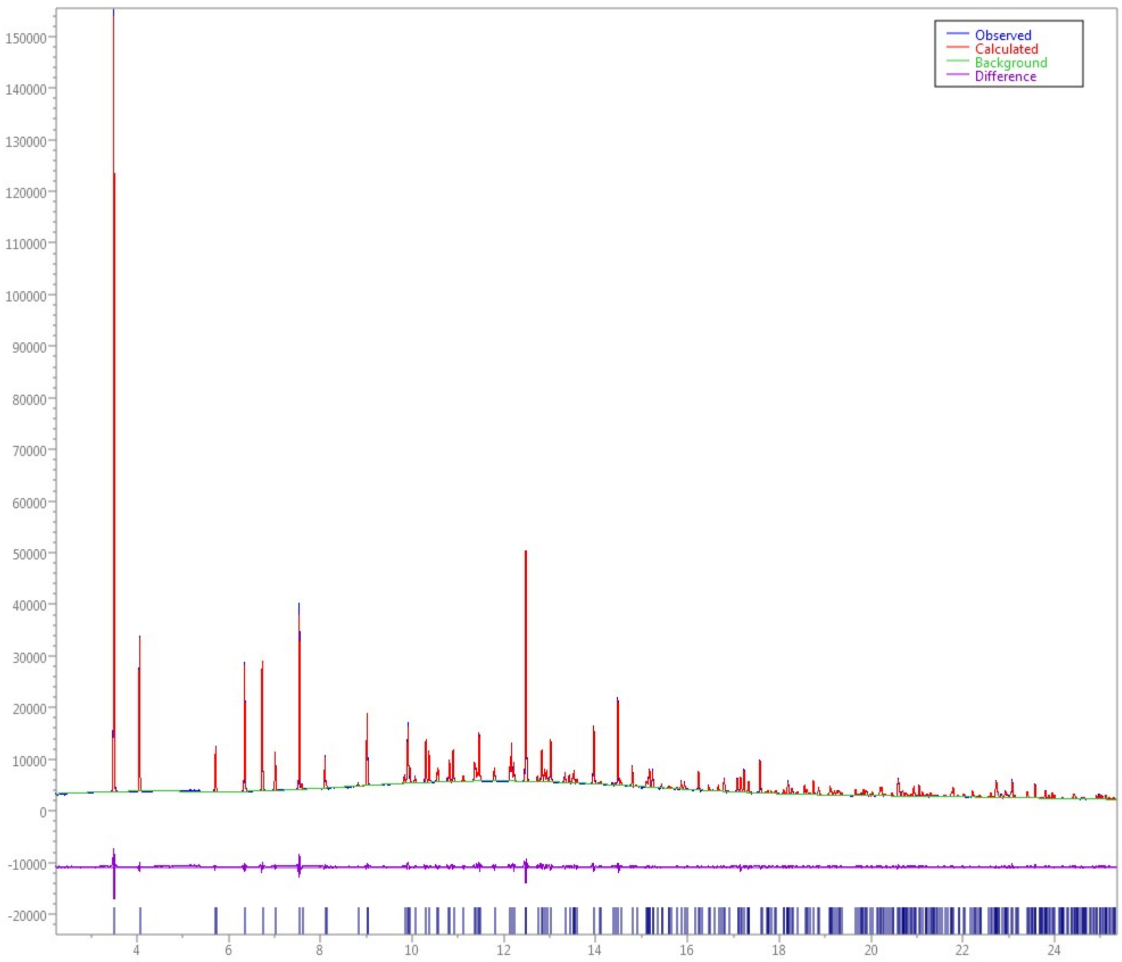

Figure S 2. The calculated pattern obtained from the extracted peaks (red) fitted against the experimentally obtained powder pattern of *cis*-Mg(dhbq)(H_2O)$_2$ (blue). The difference is shown in purple.

Air dried *cis*-$Mg(dhbq)(H_2O)_2$ crankshaft chains

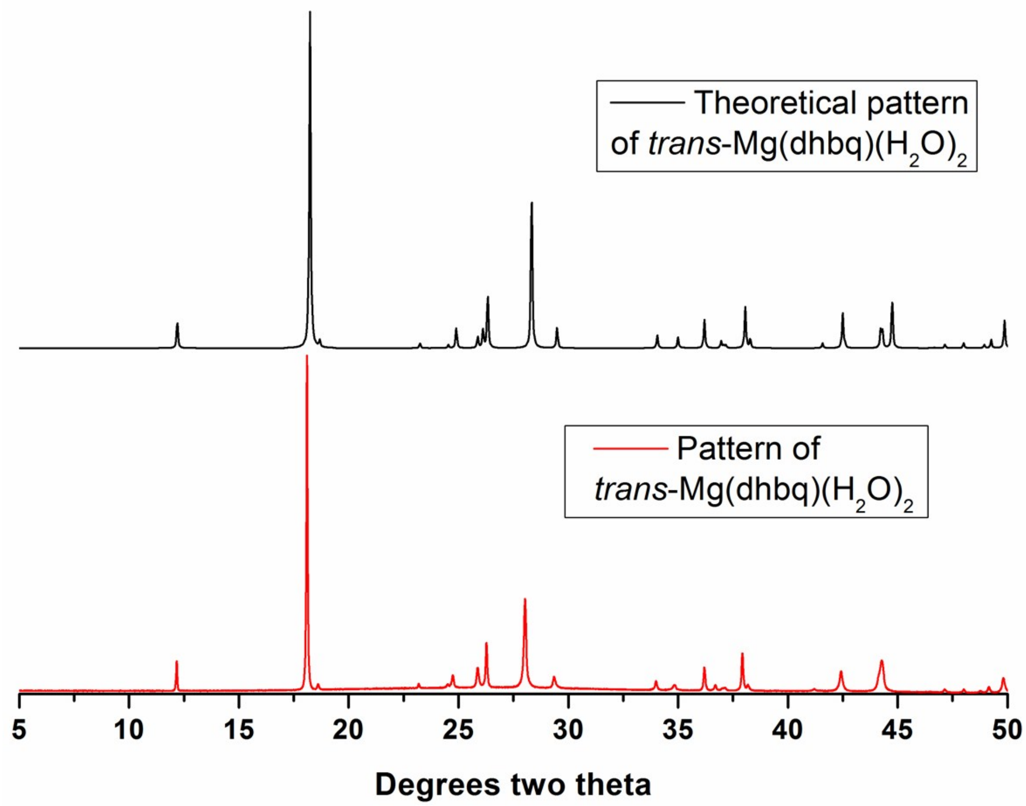

Figure S 3: Powder pattern of *trans*-$Mg(dhbq)(H_2O)_2$ obtained from an air dried sample of *cis*-$Mg(dhbq)(H_2O)_2$ (red) and the powder pattern generated from the single crystal data of *trans*-$Mg(dhbq)(H_2O)_2$ strips (black).

Table S 2. Unit cell parameters extracted from the pattern of air dried *cis*-$Mg(dhbq)(H_2O)_2$

M20 score	91.0
System	Monoclinic
a (Å)	6.887
b (Å)	7.662
c (Å)	7.862
β °	112.602
Vol (Å^3)	383.07
Rwp (%)	4.008
Rp	2.545

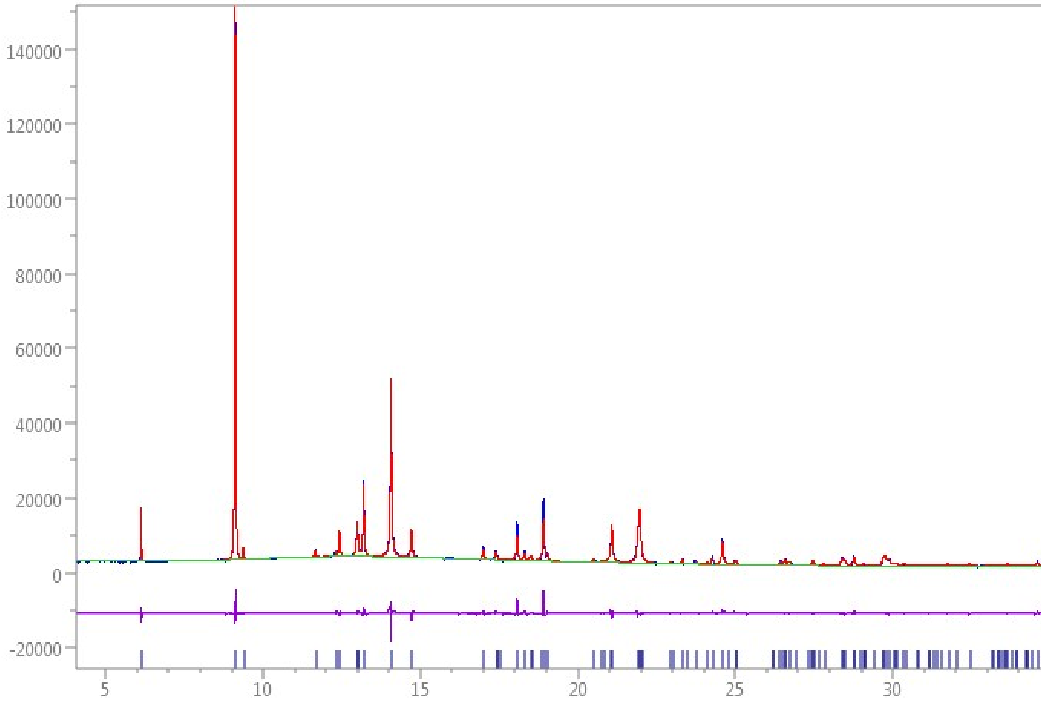

Figure S 4: The calculated pattern obtained from the extracted peaks (red) fitted against the experimentally obtained powder pattern of air dried *cis*-Mg(dhbq)(H_2O)$_2$ (blue).

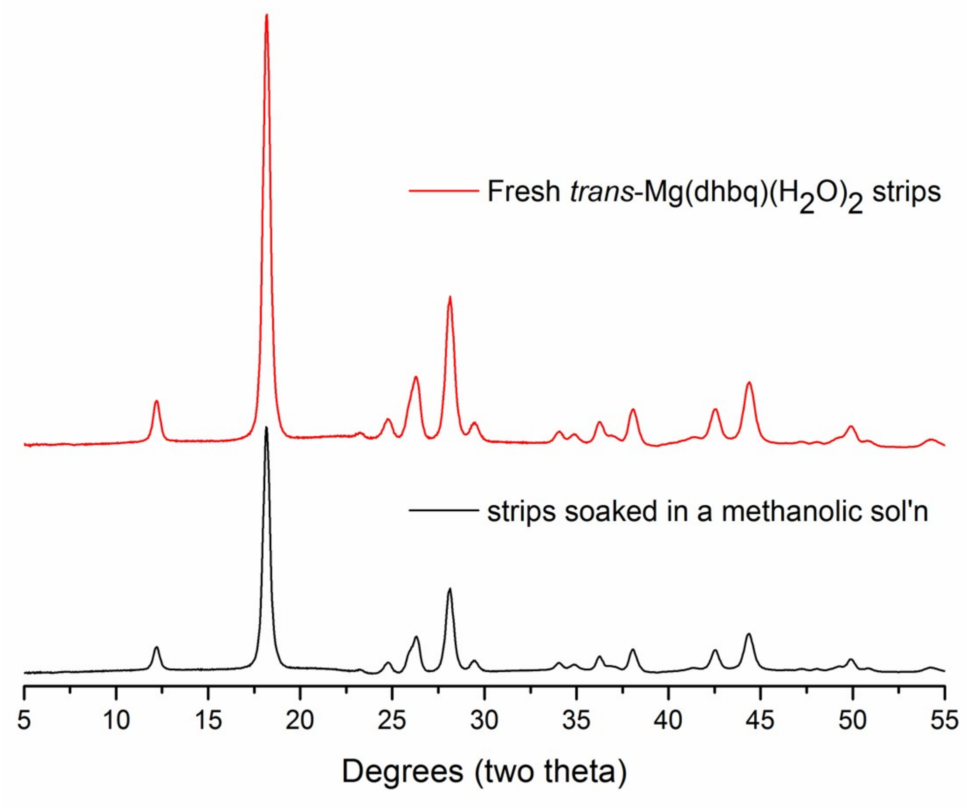

Figure S 5. X-ray powder patterns of a fresh sample of *trans*-Mg(dhbq)(H_2O)$_2$ strips (red line) and a sample of *trans*-Mg(dhbq)(H_2O)$_2$ strips soaked in a methanolic solution.

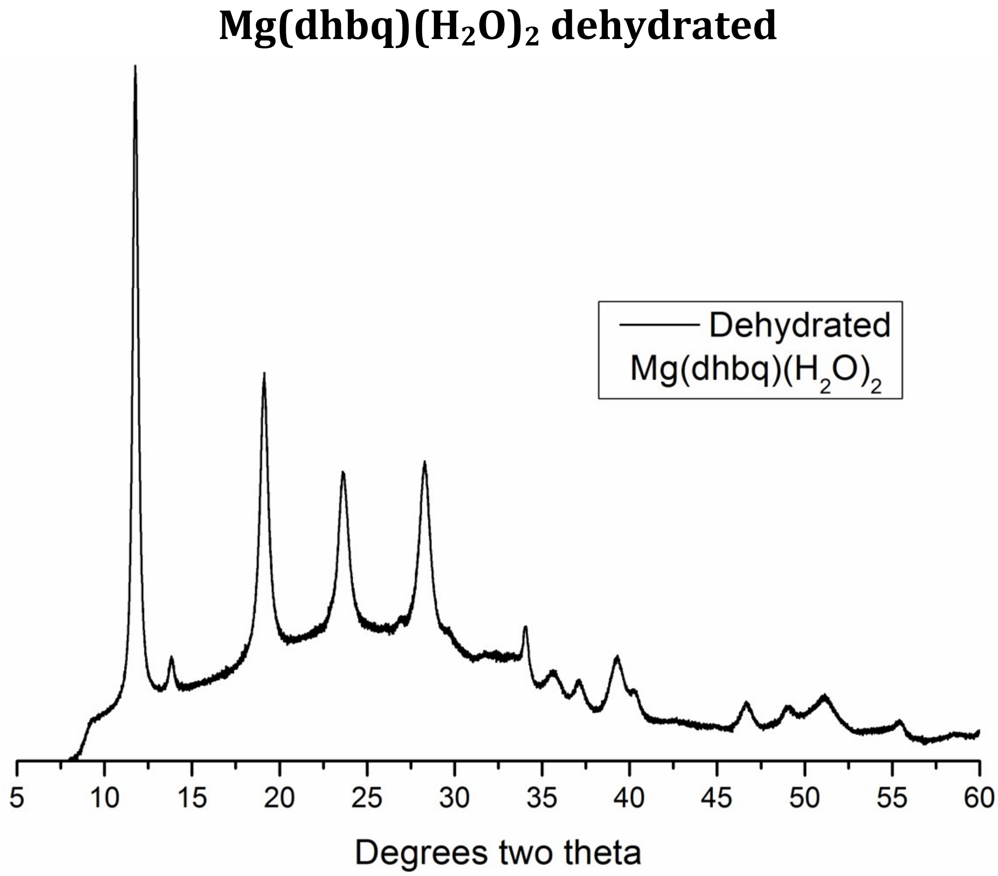

Figure S 6. A powder pattern of a sample of *trans*-Mg(dhbq)(H_2O)$_2$ which had been heated so as to remove the coordinated water molecules.

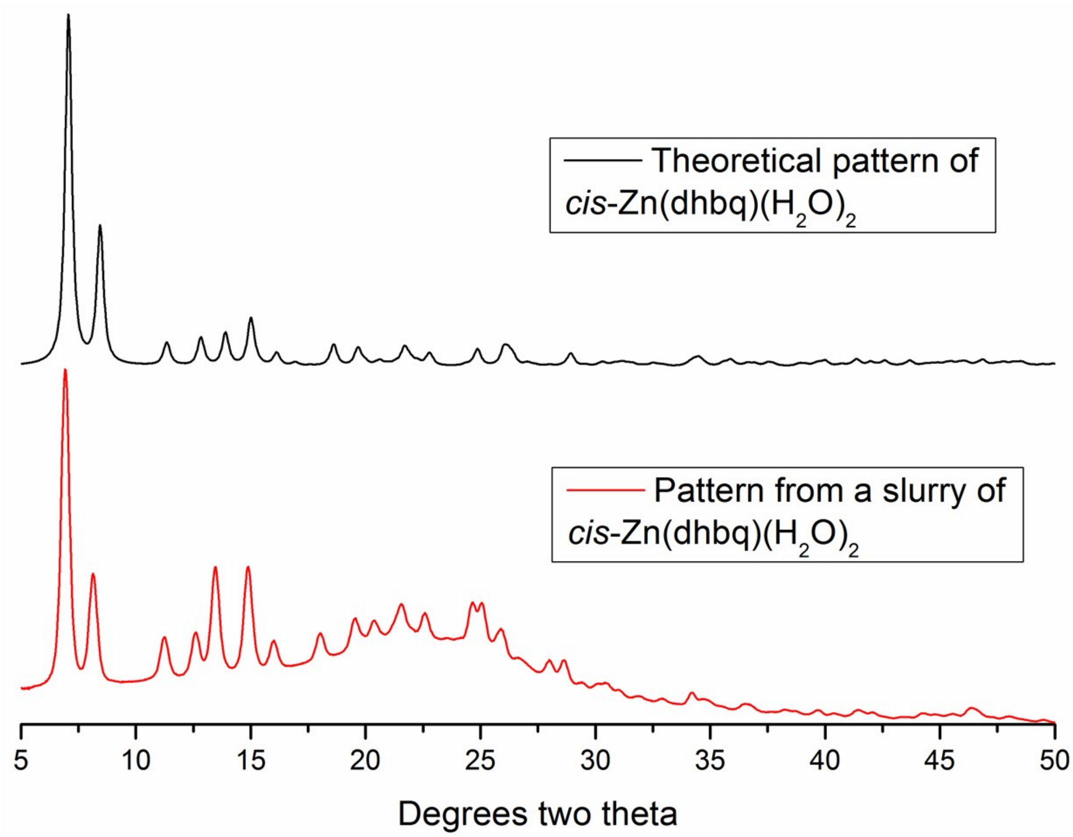

Figure S 7. Powder patterns of a slurry of *cis*-Zn(dhbq)(H_2O)$_2$ (red) and the powder pattern generated from the single crystal data of *cis*-Zn(dhbq)(H_2O)$_2$ (black).

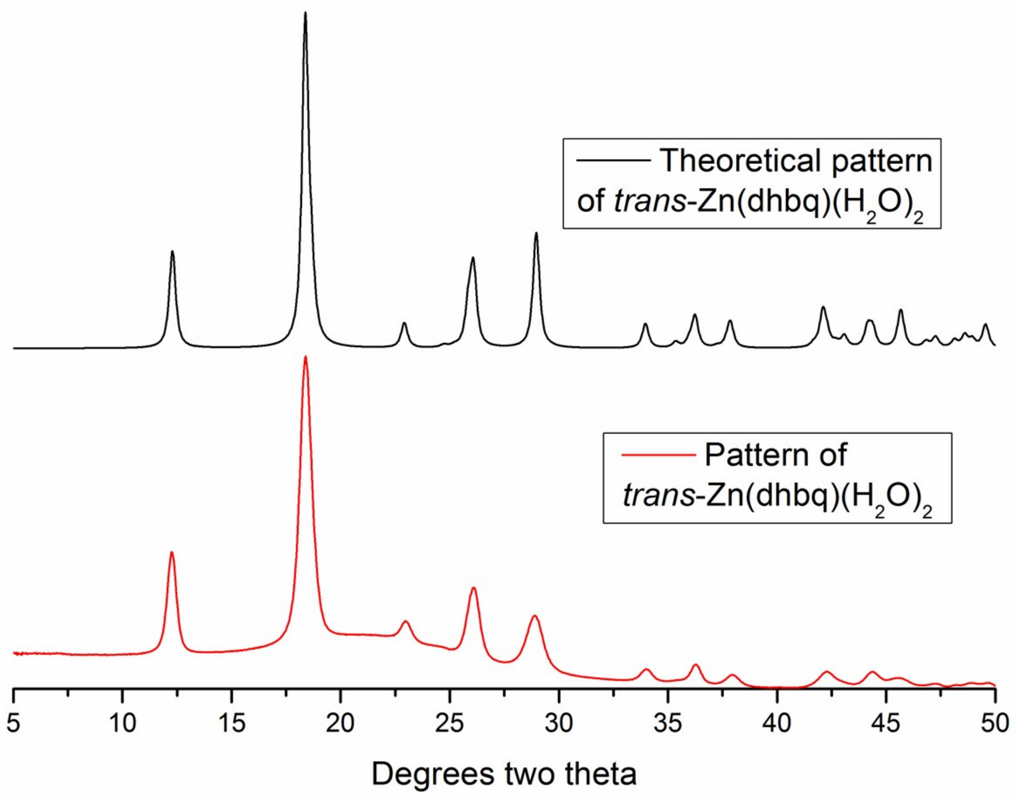

Figure S 8. Powder pattern of *trans*-Zn(dhbq)(H_2O)$_2$ obtained from an air dried sample of *cis*-Zn(dhbq)(H_2O)$_2$ (red) and the powder pattern generated from the single crystal data of *trans*-Zn(dhbq)(H_2O)$_2$ strips (black).

Zn(dhbq) dehydrated

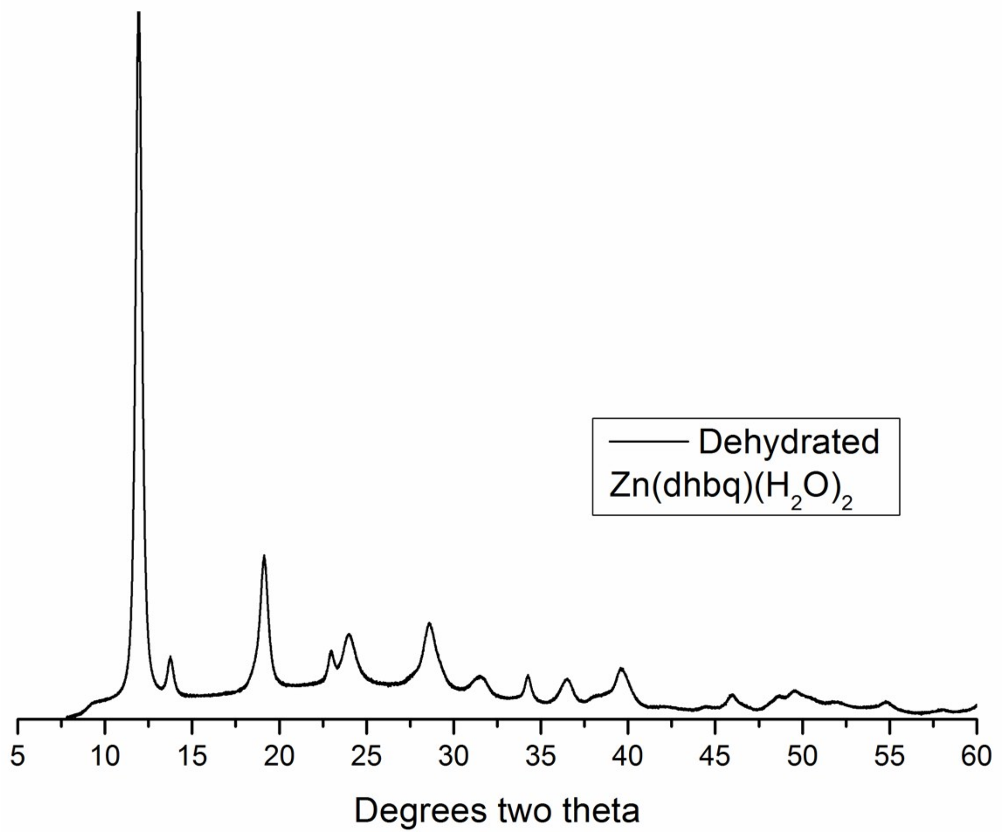

Figure S 9: A powder pattern of a sample of *trans*-Zn(dhbq)(H_2O)$_2$ which had been heated so as to remove the coordinated water molecules.

S.3 TGA studies

Thermogravimetric analyses were performed using a METTLERTGA/SDTA851 apparatus.

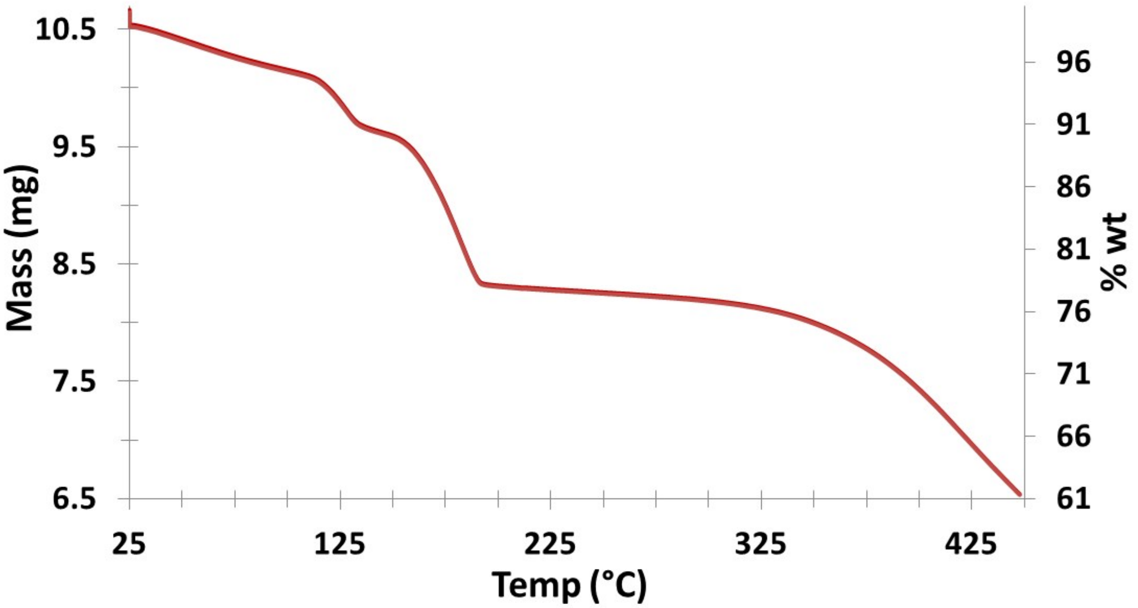

Figure S 10: TGA trace for an air dried sample of *trans*-Mg(dhbq)(H_2O)$_2$.

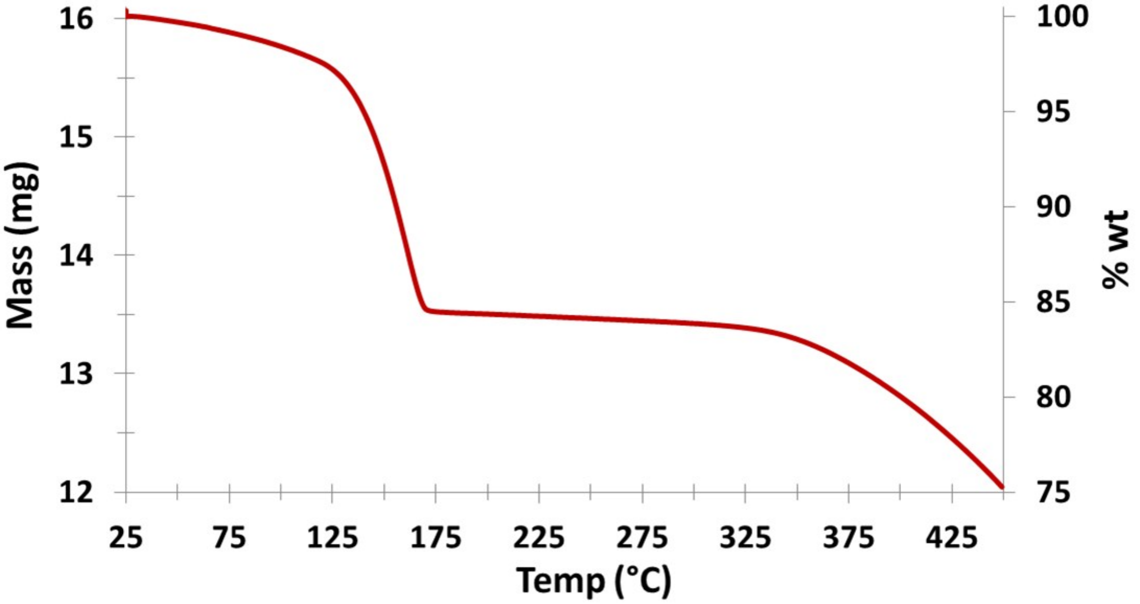

Figure S 11: TGA trace for an air dried sample of *trans*-Zn(dhbq)(H_2O)$_2$.

S.4 Infrared spectra

Infrared spectra were collected on a Bruker Tensor-24 instrument. Spectra were initially collected on freshly prepared samples of *trans*-Mg(dhbq)(H_2O)$_2$ and *trans*-Zn(dhbq)(H_2O)$_2$ which were then heated at 200 °C overnight. Samples were analyzed as KBr disks.

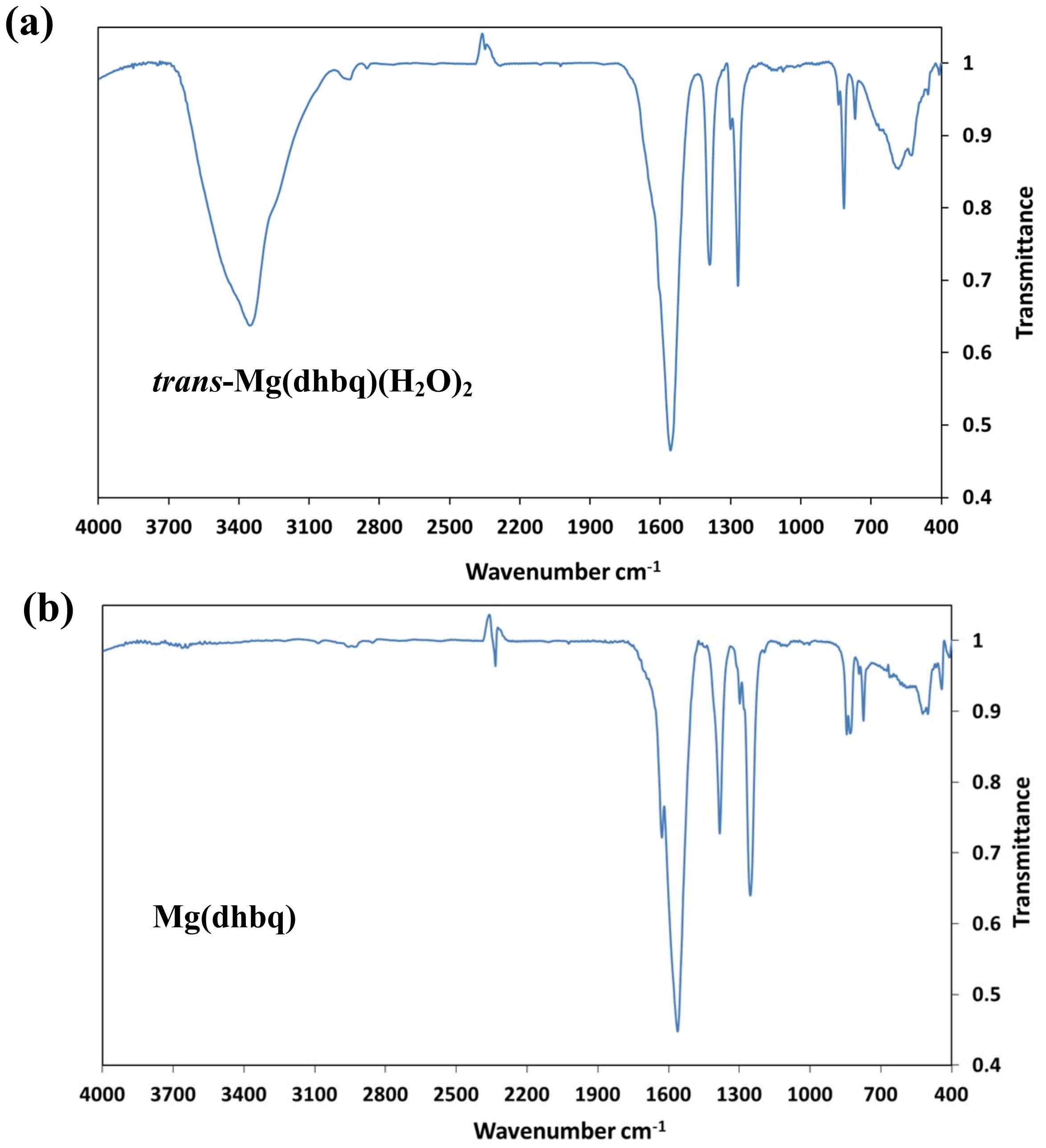

Figure S 12. Infrared spectra of (a) *trans*-Mg(dhbq)(H_2O)$_2$ and (b) Mg(dhbq).

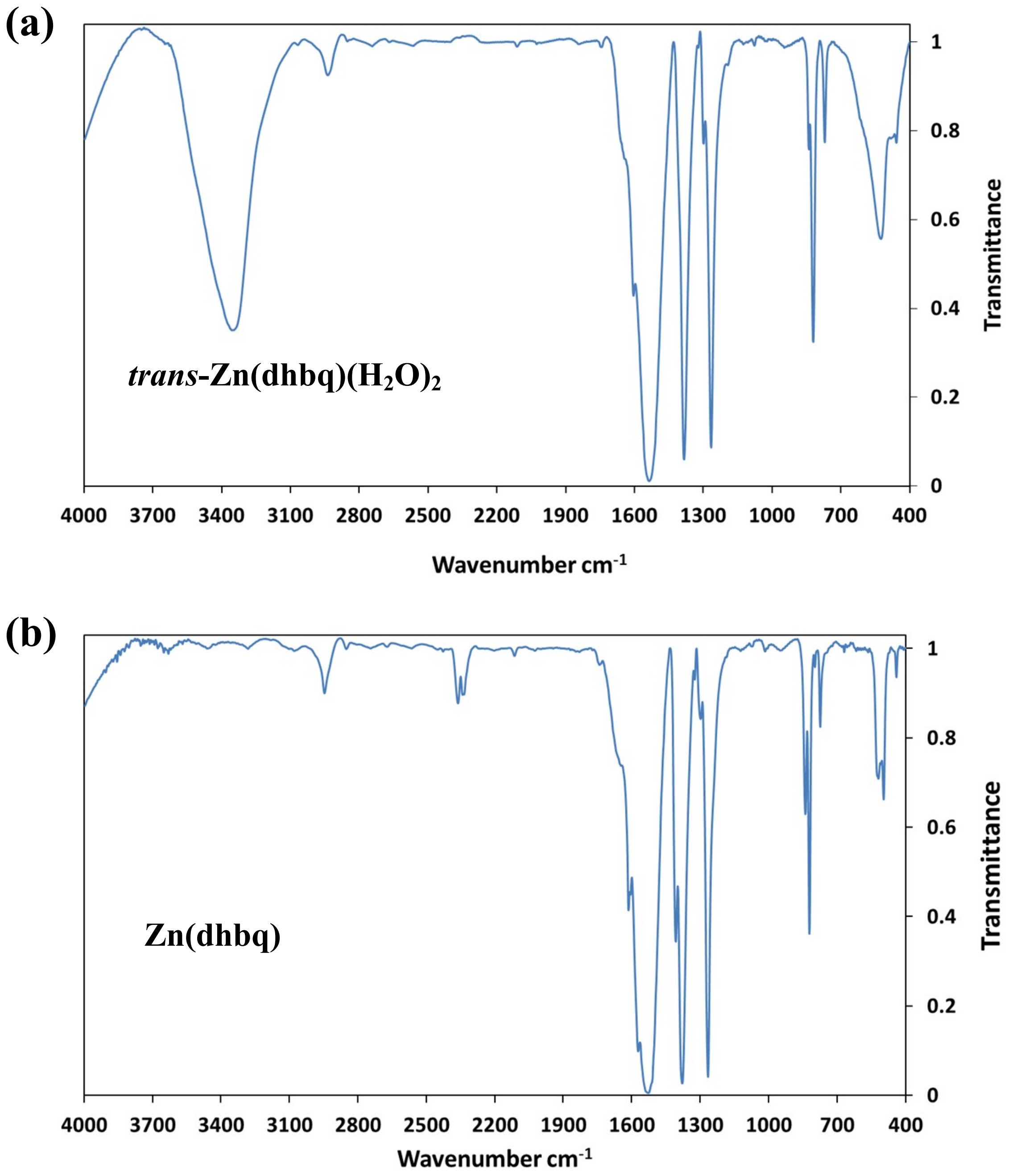

Figure S 13. Infrared spectra of (a) *trans*-Zn(dhbq)(H_2O)$_2$ and (b) Zn(dhbq).

S.5 Gas sorption studies

General Procedures

The following relate to gas sorption studies undertaken on samples of Mg(dhbq) and Zn(dhbq).

Gas sorption data were measured using a Sieverts-type BELsorp-HP automatic gas sorption apparatus (BEL Japan Inc.). Ultra-high purity CH_4, CO_2, H_2, He and N_2 used for sorption studies were purchased from BOC or Air Liquide.

Non-ideal gas behaviour at high pressures of each gas at each measurement and reference temperature was corrected for. Source data were obtained from the NIST fluid properties website. [R8]

During measurements, sample compartment temperatures ranging from 258 – 298 K were controlled by a Julabo F25-ME chiller/heater that recirculated fluid at +/- 0.1 C through a capped, jacketed stainless steel flask kept within a polystyrene foam box. A calibrated external Pt100 temperature probe monitored the flask temperature. Low temperature sorption measurements employed a cryogen level controller (BEL Japan) to maintain the liquid N_2 or Ar level around the stem of the sample compartment within 1-2 mm. Prior to gas sorption measurements, samples were kept at the measurement temperature for a minimum of 1 hr after the desired temperature had been achieved to allow full thermal equilibrium to be attained before data collection began.

Enthalpies of sorption were calculated using a least-squares fitting of a virial-type thermal adsorption equation that modelled ln(P) as a function of amount of surface excess of gas sorbed over all measurement temperatures. [R9]. Optimised virial coefficients and R^2 values for Mg(dhbq) and Zn(dhbq) and are given in Table S1 and S2 respectively.

Horvath Kawazoe plots were generated by the BELmaster software using 77 K N_2 isotherm data.

Mg(dhbq) gas sorption studies

The following data relate to gas sorption studies on a sample of *cis*-Mg(dhbq)(H_2O)$_2$ that had undergone dehydration under vacuum at a temperature of 180°C overnight to form Mg(dhbq).

Table S3. Optimised virial coefficients for modelling excess gas adsorption on Mg(dhbq).

Gas	**H_2**	**CO_2**	**CH_4**
Temp /K	77, 87	258, 273.2	258, 273.2 298.2
a0	-1127.4	-4465.4	-3106.7
a1	-2.06814	-119.154	-44.3737
a2	11.018	296.3457	120.2939
a3	-0.10804	-157.209	-42.4145
a4	-0.30257	42.51043	6.32203
a5	0.053469	-3.95022	0.338293
b	12.14916	16.79027	15.11352
R^2	0.9995526	0.99968444	0.99904762

Mg(dhbq) Hydrogen sorption studies

a)

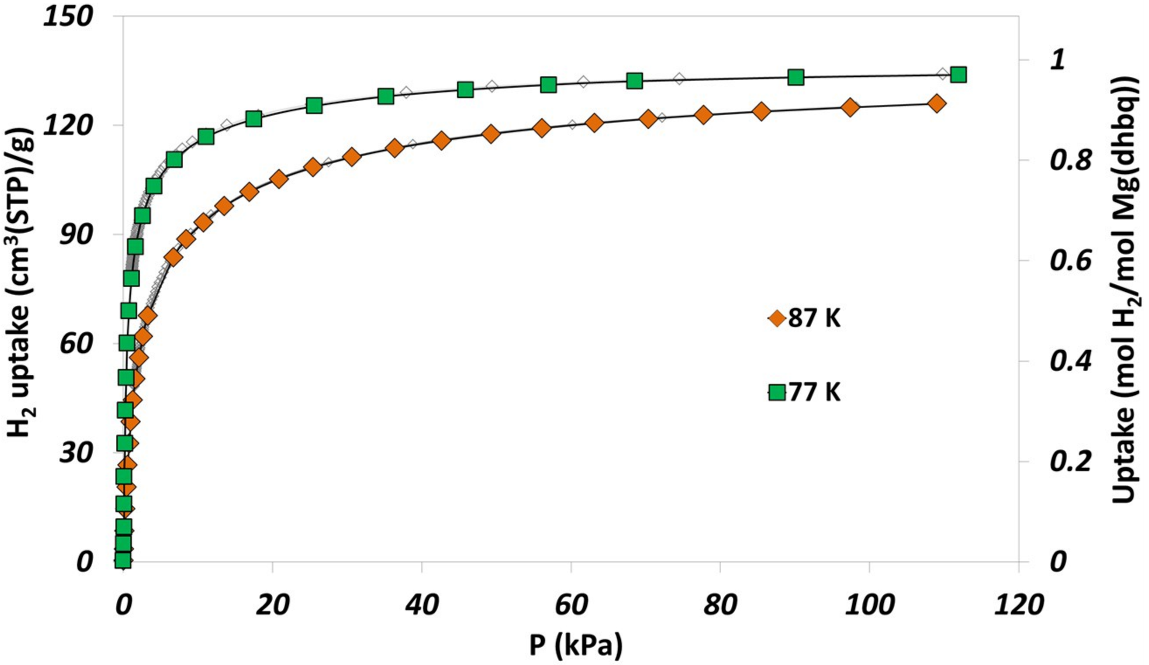

b)

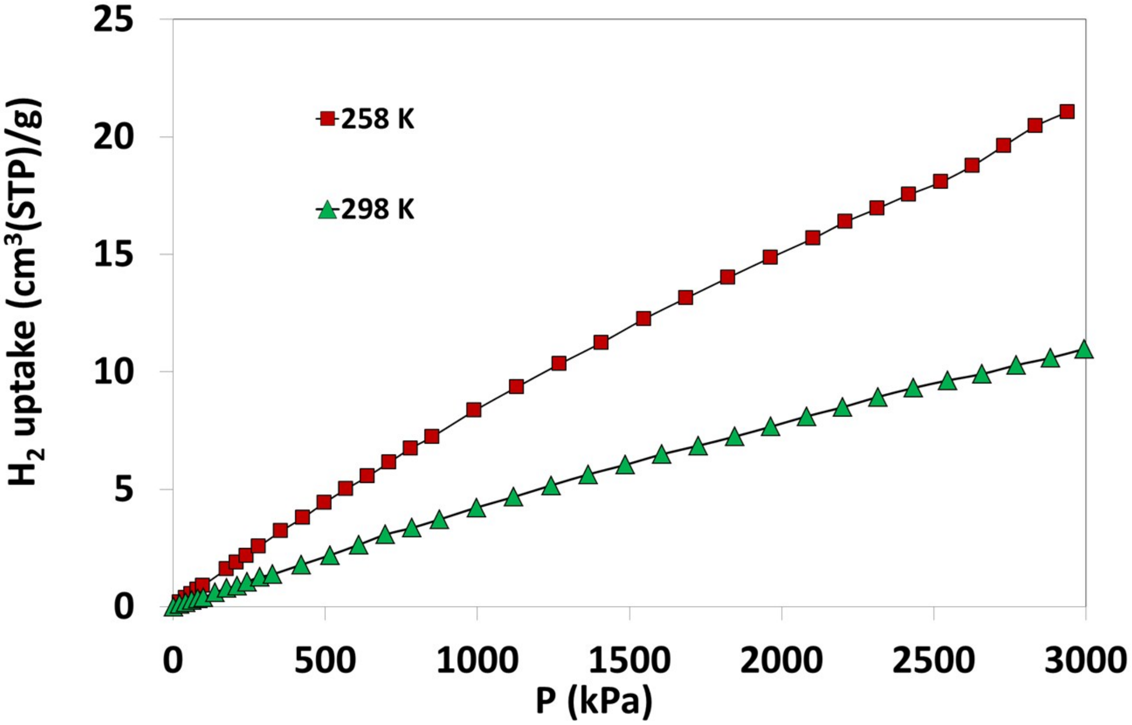

c)

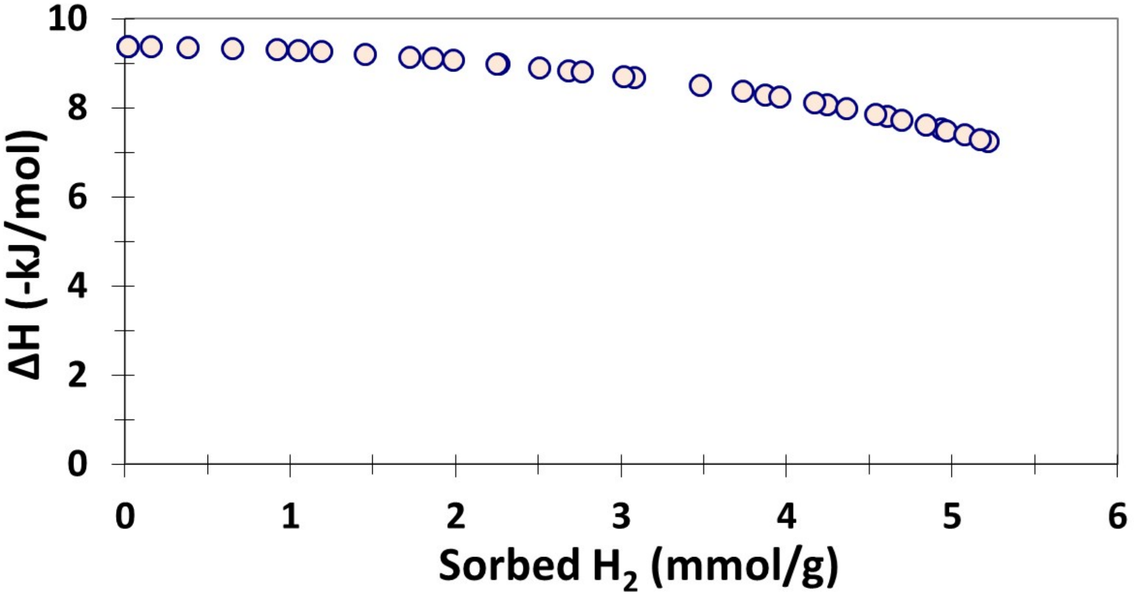

Figure S 14: a) H_2 sorption isotherms measured at 77 (green squares) and 87 K (orange diamonds), desorption paths are presented by hollow data points. b) H_2 sorption isotherms at 258 and 298 K. c) H_2 sorption enthalpy versus H_2 sorbed.

Mg(dhbq) Nitrogen sorption studies

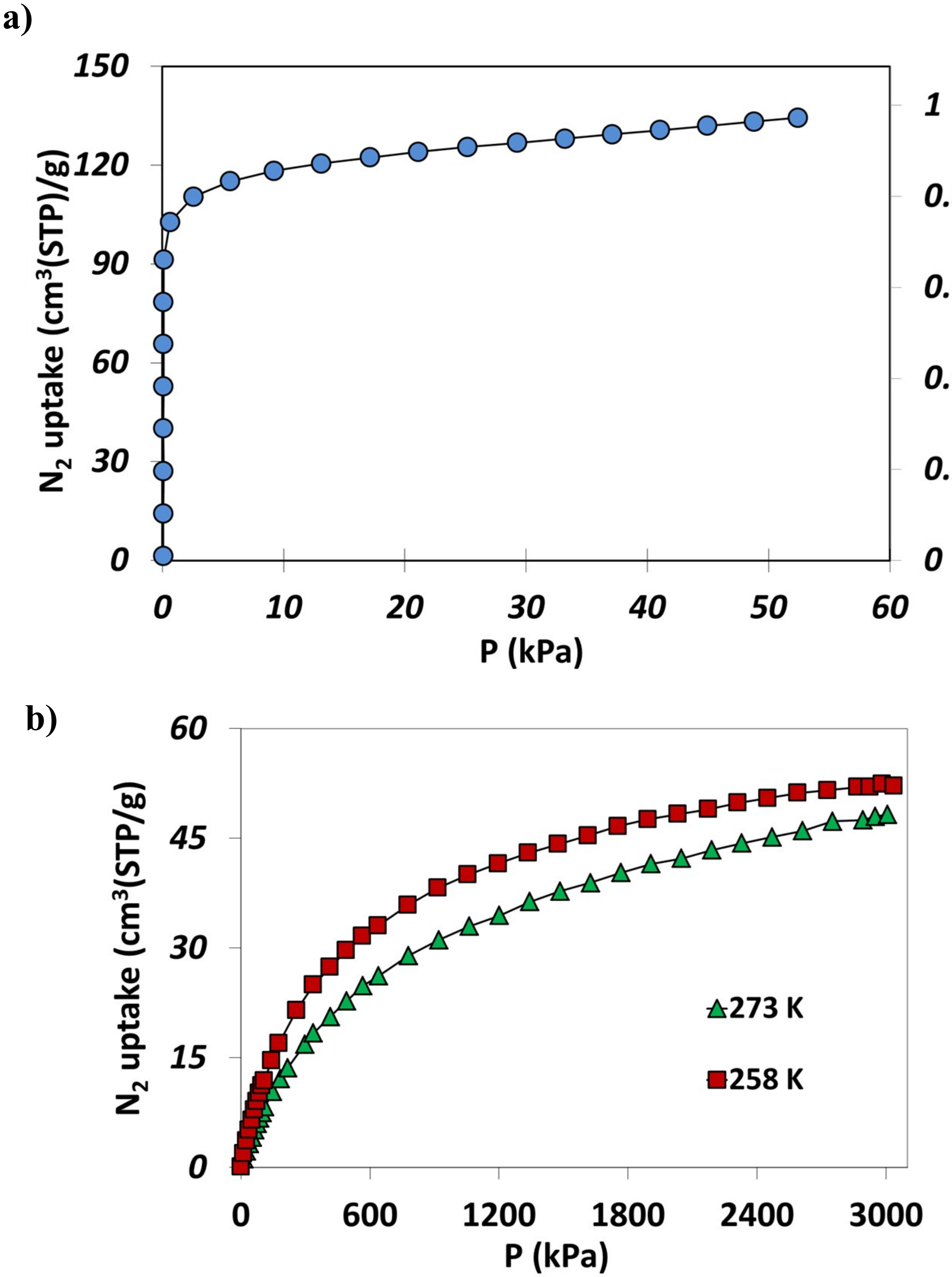

Figure S 15: a) A N_2 sorption isotherm measured at 77 K. b) N_2 sorption isotherms measured at 258 (red squares) and 273 K (green triangles).

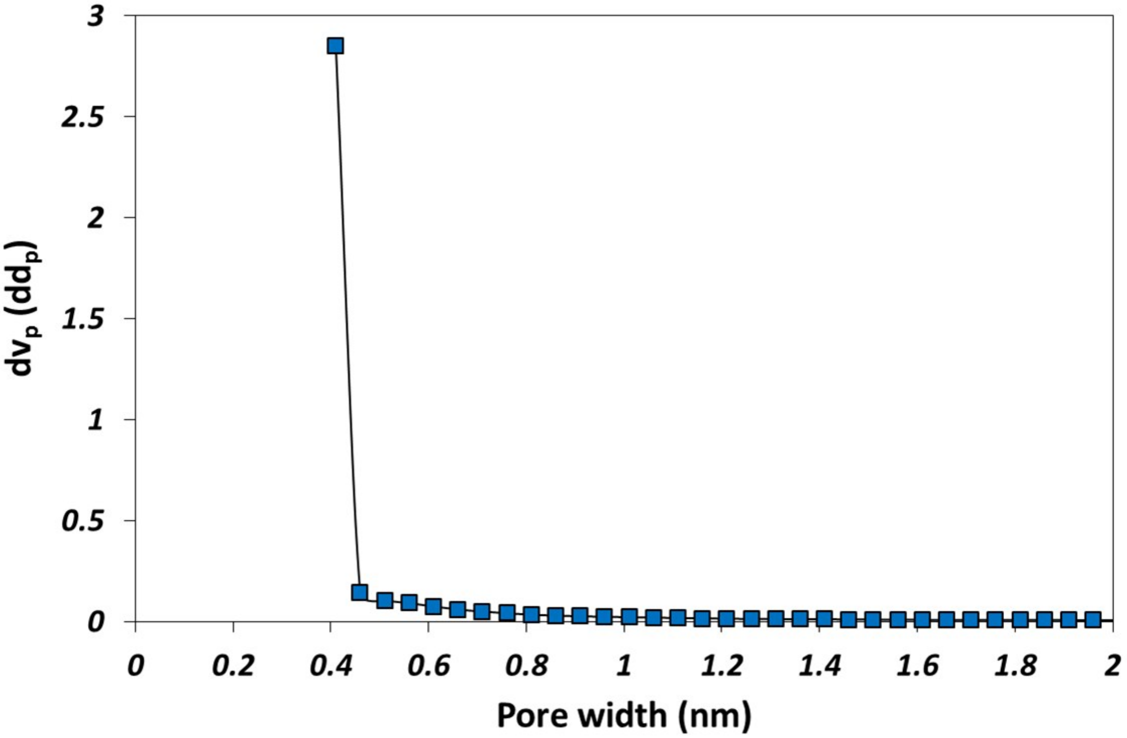

Figure S 16. Mg(dhbq) HK plot obtained from 77 K N_2 isotherm data.

Mg(dhbq) carbon dioxide sorption studies

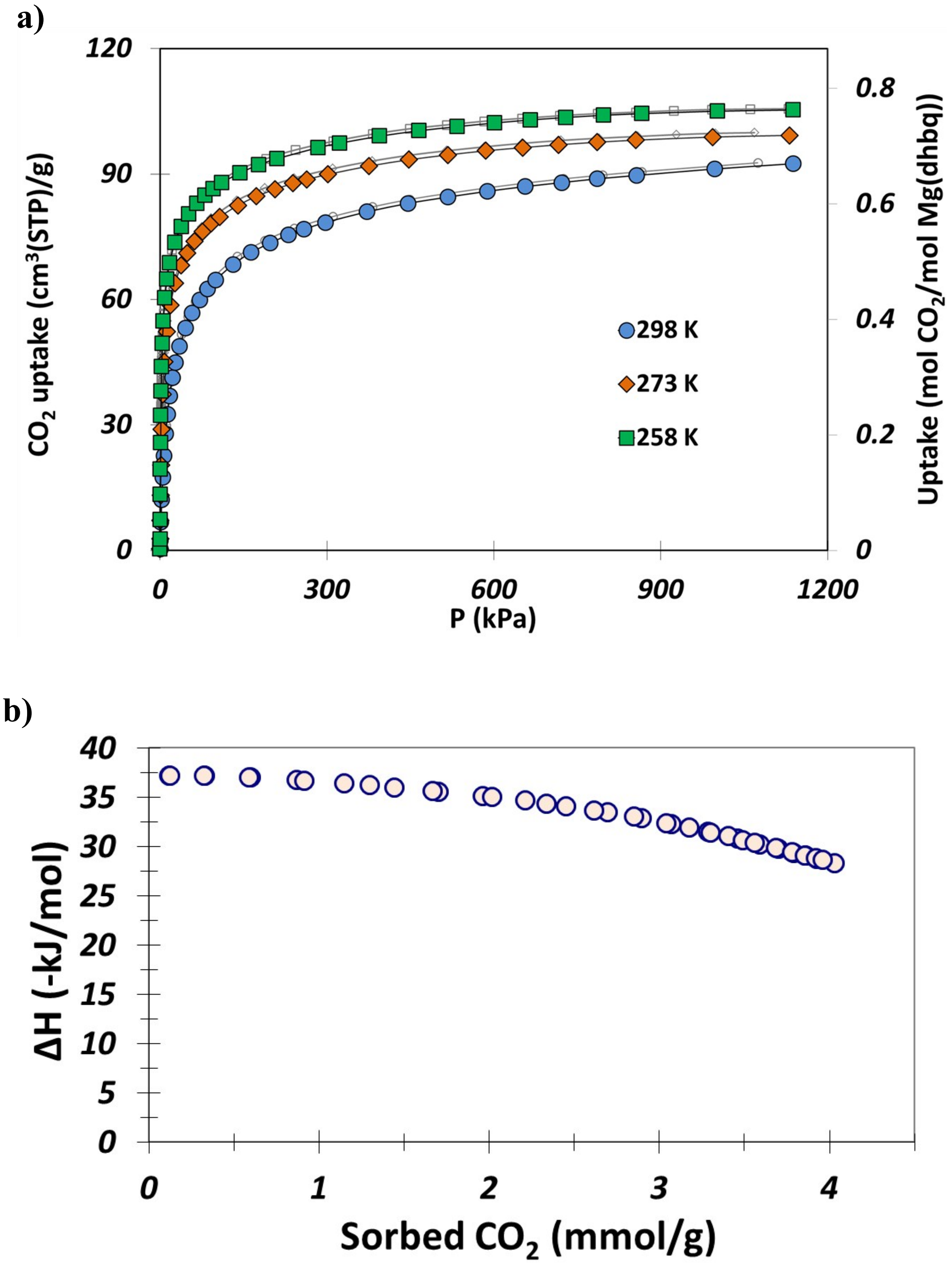

Figure S 17: a) CO_2 sorption isotherms measured at 258 (green squares), 273 (orange diamonds) and 298 K (blue circles), desorption curves are presented with hollow makers. b) CO_2 Sorption enthalpy versus CO_2 sorbed.

Mg(dhbq) methane sorption studies

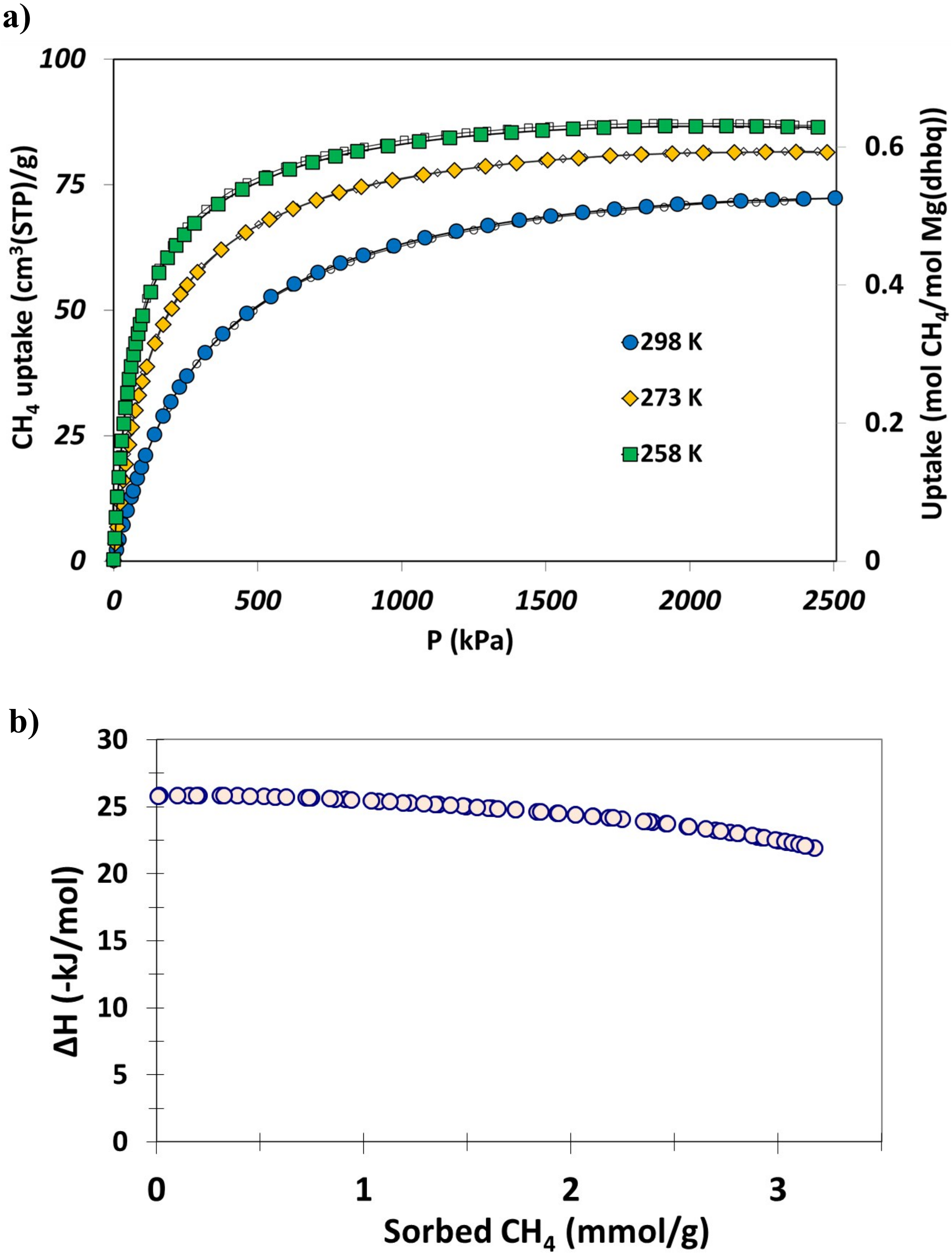

Figure S 18: a) CH_4 sorption isotherms measured at 258 (green squares), 273 (orange diamonds) and 298 K (blue circles), desorption curves are presented with hollow markers. b) CH_4 sorption enthalpy versus CH_4 sorbed.

Zn(dhbq) gas sorption studies

The following data relate to gas sorption studies on a sample of *trans*-Zn(dhbq)(H_2O)$_2$ that had undergone dehydration under vacuum at a temperature of 180°C overnight to form Zn(dhbq).

Table S4. Optimised virial coefficients for modelling excess gas adsorption on Zn(dhbq).

Gas	**H_2**	**CO_2**	**CH_4**
Temp /K	77, 87	258, 273, 298	258, 273
a0	-1096.07	-4326.37	-3209.58
a1	121.0972	-141.351	63.52883
a2	-100.267	358.4645	78.63564
a3	43.34803	--190.892	-20.8813
a4	-7.63809	66.18738	-0.70347
a5	0.584667	-7.96787	2.587828
b	11.45391	16.59971	15.25754
R^2	0.994699303	0.99978908	0.99980881

Zn(dhbq) hydrogen sorption studies

a)

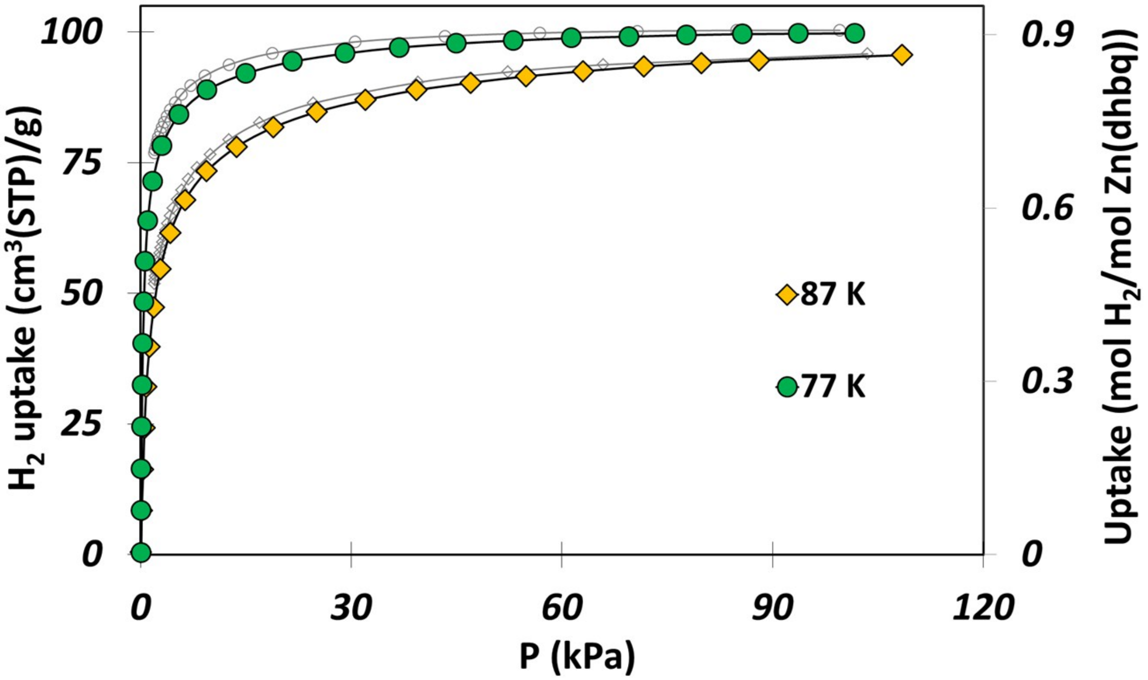

b)

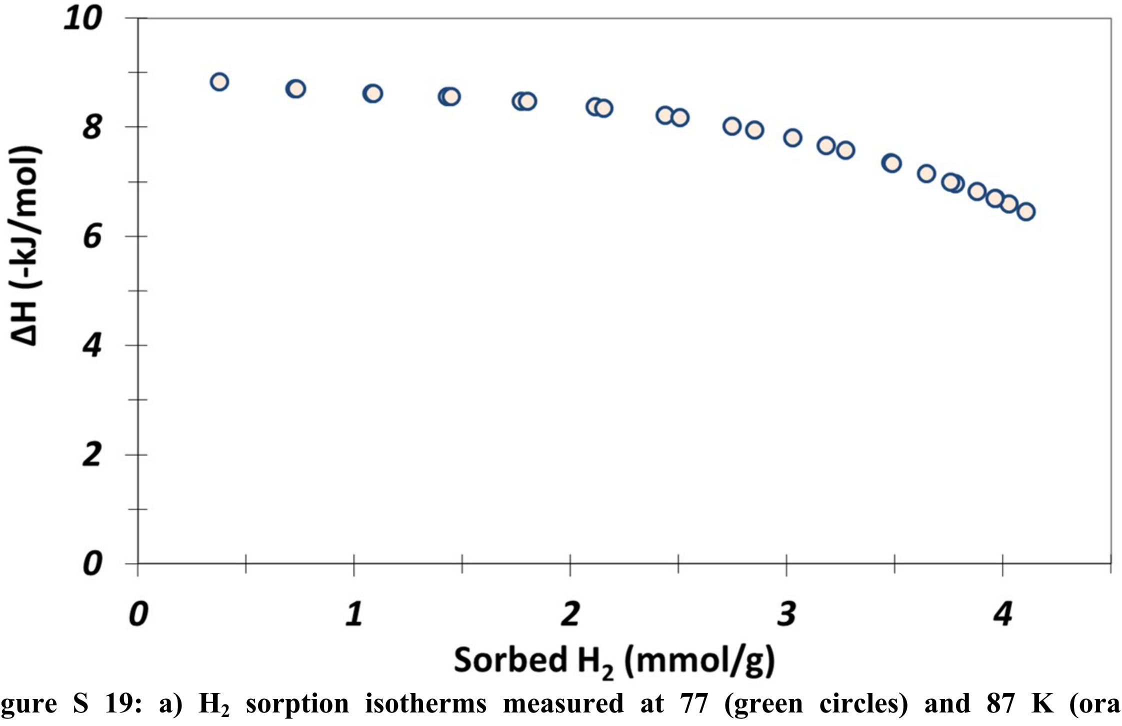

Figure S 19: a) H_2 sorption isotherms measured at 77 (green circles) and 87 K (orange diamonds), desorption curves are presented with hollow markers. b) H_2 sorption enthalpy versus H_2 sorbed.

Zn(dhbq) nitrogen sorption studies

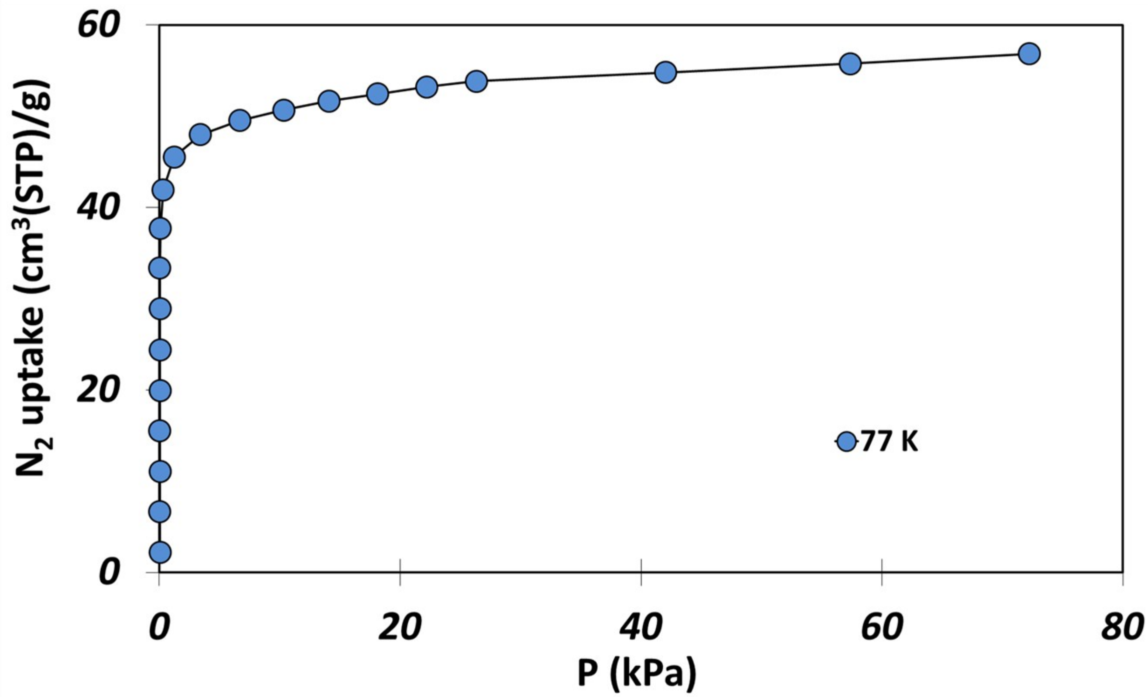

Figure S 20: A N_2 sorption isotherm measured at 77 K.

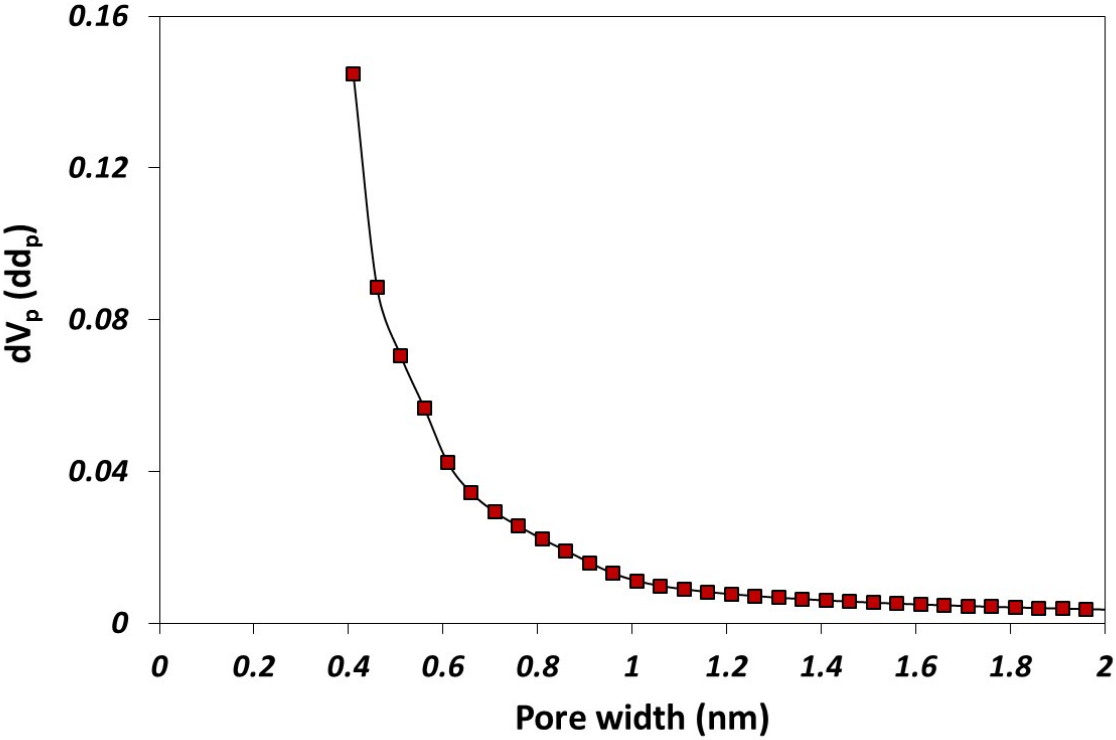

Figure S 21. Zn(dhbq) HK plot obtained from 77 K N_2 isotherm data.

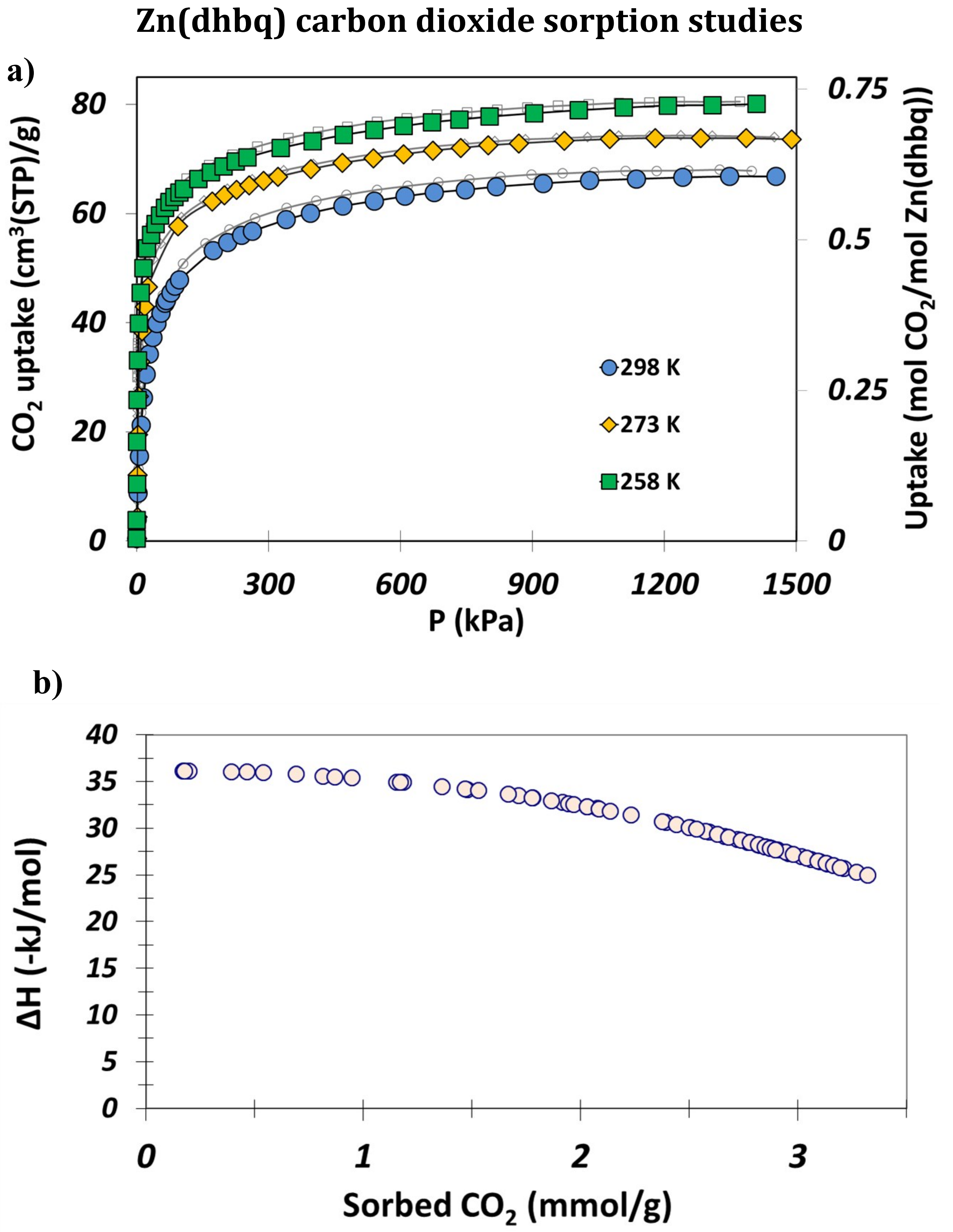

Figure S 22: CO$_2$ sorption isotherms measured at 258 (green squares), 273 (orange diamonds) and 298 K (blue circles), desorption curves are presented with hollow makers. b) CO$_2$ Sorption enthalpy versus CO$_2$ sorbed.

Zn(dhbq) methane sorption studies

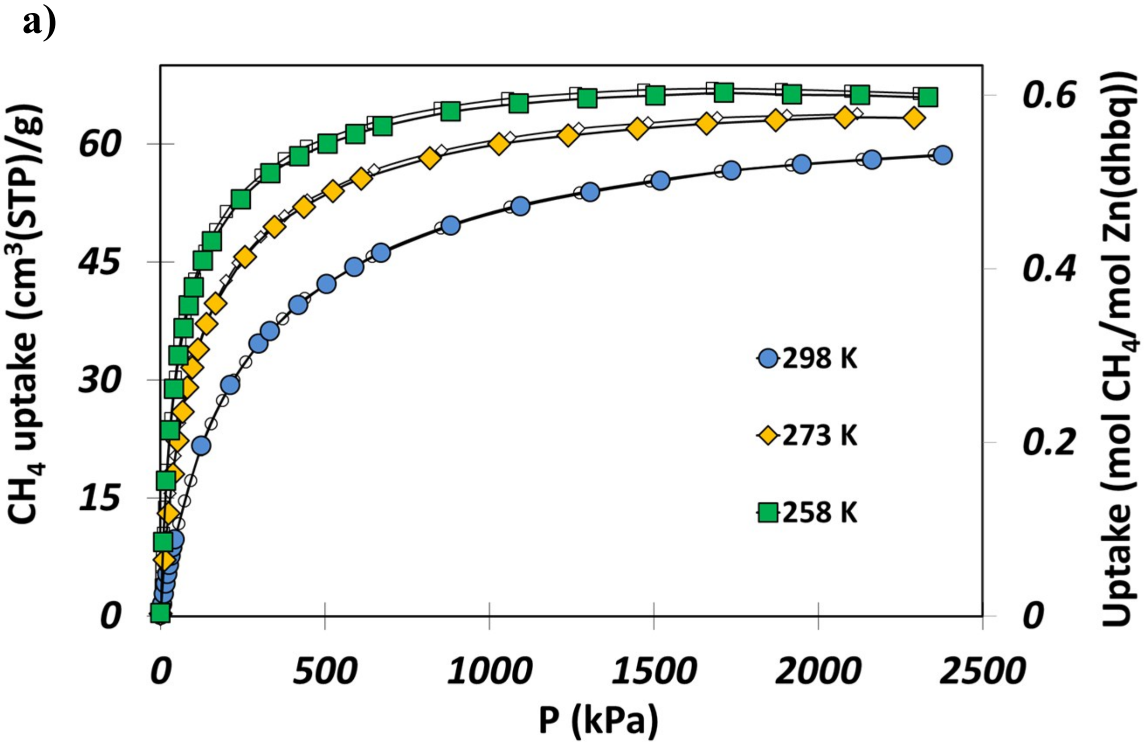

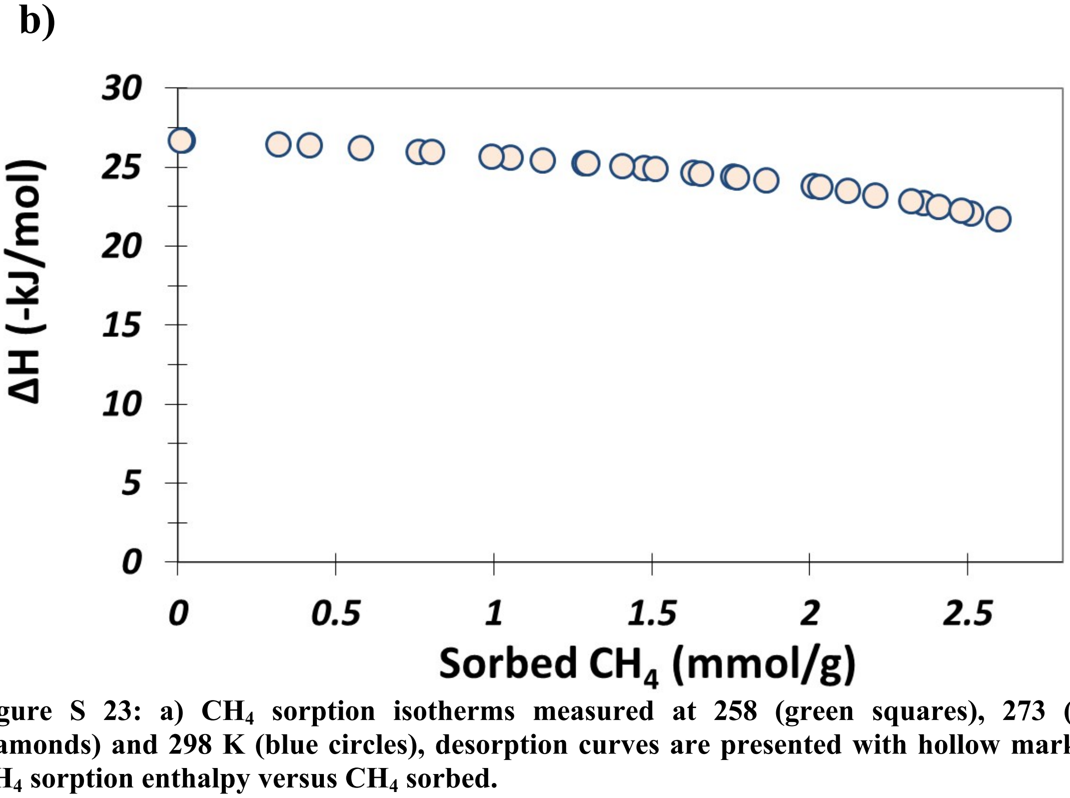

Figure S 23: a) CH$_4$ sorption isotherms measured at 258 (green squares), 273 (orange diamonds) and 298 K (blue circles), desorption curves are presented with hollow markers. b) CH$_4$ sorption enthalpy versus CH$_4$ sorbed.

S. 6 References

[R1] Weider, P.R., Hegedus, L.S., Asada, H., D'Andreq, S. V., *J. Org. Chem.*, 1985, **50**, 4276

[R2] Farrugia, L. J, *Journal of Applied Crystallography* **2012**, *45*, 849-854.

[R3] Sheldrick, G. M, *Acta Crystallographica Section A: Foundations of Crystallography* **2007**, *64* (1), 112-122.

[R4] Spek, A. L, *Acta Cryst. Section D: Biological Crystallography* **2009**, *65*, 148-155.

[R5] Wallwork, K. S., Kennedy, B. J., Wang, D., The high resolution powder diffraction beamline for the Australian Synchrotron, *AIP Conference Proceedings*. **879**, 879-882, (2007).

[R6] Schmitt, B., C. Bronnimann, et al. (2003). "Mythen Detector System." Nuclear Instruments and Methods in Physics Research A **501**: 267 - 272.

[R7] Altomare, A., Cuocci, C., Giacovazzo, C., Moliterni, A., Rizzi, R., Corriero N., and Falcicchio, A. , "EXPO2013: a kit of tools for phasing crystal structures from powder data", *J. Appl. Cryst.* (2013). **46**, 1231-1235

[R8] http://webbook.nist.gov/chemistry/fluid/

[R9] Czepirski, L., Jagiello, J., *Chem. Eng. Sci*. 1989, **44**, 797–801